

Preparation and characterization of activated

by Wara Dyah Pita Rengga

Submission date: 14-May-2023 08:28PM (UTC+0700)

Submission ID: 2092675686

File name: Preparation_and_characterization_of_activated.pdf (807.75K)

Word count: 4450

Character count: 23415

PAPER • OPEN ACCESS

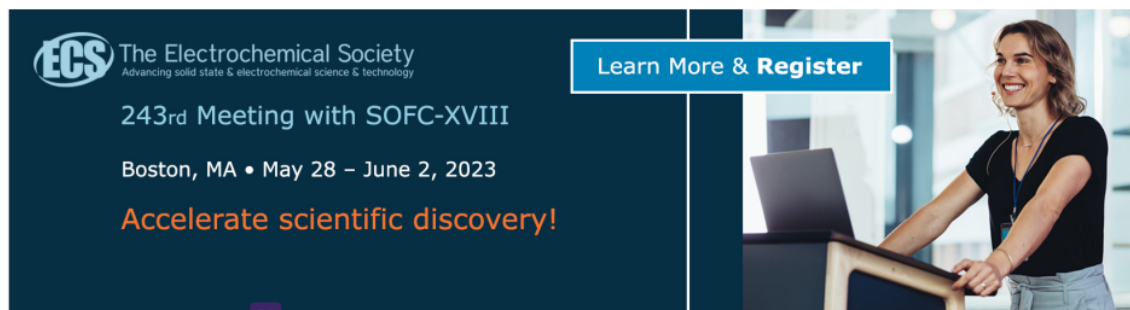
Preparation and characterization of activated carbon derived from the bovine bone doped urea as an electrode material

6
To cite this article: N Khoirina *et al* 2022 *IOP Conf. Ser.: Earth Environ. Sci.* **969** 012040

6
View the [article online](#) for updates and enhancements.

You may also like

- 9
- [Boron, Nitrogen-Doped Porous Carbon Derived from Biowaste Orange Peel as Negative Electrode Material for Lead-Carbon Hybrid Ultracapacitors](#)
Sadananda Muduli, Vangapally Naresh and Surendra K. Martha
- 8
- [A Study on the Thermal Behavior of an Ultracapacitor Module Comprising 136 Cells](#)
Sung June Park, Jaeshin Yi, Chee Burm Shin et al.
- [Storage and separation of methane and carbon dioxide using platinum- decorated activated carbons treated with ammonia](#)
Mohamed F Aly Aboud, Zeid A ALOthman and Abdulaziz A Bagabas



The Electrochemical Society
Advancing solid state & electrochemical science & technology

243rd Meeting with SOFC-XVIII
Boston, MA • May 28 – June 2, 2023
Accelerate scientific discovery!

Learn More & Register

The advertisement features a dark blue background on the left with white and orange text. On the right, there is a photograph of a woman with blonde hair, wearing a black top and light-colored pants, smiling and looking at a laptop on a desk in a modern office setting.

Preparation and characterization of activated carbon derived from the bovine bone doped urea as an electrode material

N Khoirina, A F Nugraheni, A A Alfian and W D P Rengga

Department of Chemical Engineering, Faculty of Engineering, Universitas Negeri Semarang, Kampus Sekaran, Gunungpati, Semarang, 50229, Indonesia

wdpitar@mail.unnes.ac.id

Abstract. Activated carbon was prepared as an electrode by utilizing available bovine bone waste. This material is an alternative to graphene, which still has a high price value. The aims of this study were to characterize and analyze the effect of urea on the manufacture of activated carbon as an electrode, and to analyze the performance of ultracapacitors from modified electrodes combined with several electrolytes. Urea is formulated because it has a nitrogen group in the activated carbon synthesis process. Treatment of bovine bone carbon started from size reduction and carbonization, activation with KOH. While the carbon modification process added urea (1:1, 1:2, 1:3) and continued with washing and neutralization. Activated carbon powder has hydroxyapatite, CaO, and CaOH, which maintains its macroscopic structure during combustion. On the carbon surface there are active groups such as hydroxyl, amine derivatives, phosphates. Carbon with a large surface area has nanometer-sized porosity and pore volume so that it can be used to provide space for energy storage. The results showed that the carbon added with urea (1:2) had the best characterization. The performance of the ultracapacitor was measured by its capacitance of 292 F/g and 0.1 A/g in the organic electrolyte liquid TEABF₄.

1. Introduction

Fuel consumption continues to increase, which has an impact on energy availability. Today, the most crucial thing in the energy field is energy storage for hybrid vehicles. In addition, electrical equipment and natural energy sources also play a role, such as wind, solar, fuel cells, and tidal energy [1], and energy distribution. However, the energy needed is in the form of energy storage media that accumulates in the short term, is stored for a long time, and can be reused quickly. Therefore, the role of energy storage with high performance, clean, efficient, and environmentally friendly is significant.

Energy storage can be in the form of capacitors having many components with long service life, faster charge-discharge rate, high power density, and energy storage [2] compared to Lithium batteries [3]. Part of this ultracapacitor is an electrode in the form of a high-capacitance graphene-type carbon. The selling value for this material is quite expensive because it combines a complicated preparation and manufacturing process and limited raw materials [4]. Another part of the ultracapacitor is the electrolyte, in acidic or basic solutions that produce more excellent ionic conductivity with high specific capacitance and small solution resistance. The weakness encountered is that acidic and alkaline conditions tend to be decomposed by water, limiting its energy density [5], so it is necessary to choose a neutral electrolyte [6].

The electrostatic interactions between the electrode surface and the polarized electrolyte significantly affect the energy storage capability. Specifically, the properties of electrodes such as porous carbon and electrolytes can form an electric double layer (EDLC) to produce superior power so that the electrode



Content from this work may be used under the terms of the [Creative Commons Attribution 3.0 licence](https://creativecommons.org/licenses/by/3.0/). Any further distribution of this work must maintain attribution to the author(s) and the title of the work, journal citation and DOI.

16 capacitance can be related to the surface area and polarization of the electrode [6]. It can be shown from the electrode pores that match the chemical electrolyte ions, and the electrode surface matches the solvent for the Faraday reaction [7].

The choice of biomass-based carbon should have material and energy density to increase the device's specific capacitance and working potential. Biomass that has a high density is animal bones. The bone was unique in the form of a composite matrix structure with organic, inorganic, and water content of 22%, 69%, and 9%, respectively [8]. Organic content is determined by the central carbon, while inorganic is indicated by naturally doped heteroatoms, increasing the capacitance [5]. Based on the analysis of Mohammed et al. [9], bovine bone has a reasonably high fixed carbon content of around 84.83% [9] when compared to other bones such as goat bone (82.01%) [10] at a heating temperature of more than 500°C. The higher the fixed carbon content, the higher the yield given.

Several researchers have fabricated bovine bone activated carbon biomaterials and characterized them, which have been activated to produce specific capacitance at current densities of 185 F/g at 0.5 A/g [11], 108 F/g at 9 A/g (electrolyte EMIBTI) [12], and 258 F/g at 5 A/g [7]. However, the electrodes obtained still have shortcomings, especially in the value of the resulting capacitance, which is still quite small. In addition, the pyrolysis operating temperature for carbon activation is very high (1100°C). Therefore, it is necessary to form many pores with micro size to obtain a surface area for electrochemical applications. The presence of the doping process on carbonation in the pyrolysis of bovine bone powder affects the carbon character on the storage ability [10].

The addition of nitrogen serves to form a chemical bond between carbon and the electrolyte. Electrolytes from inorganic tend to decompose so that they are transferred to neutral electrolytes and from nature. The carbon electrode (including the phosphorus content) is formed through physical and chemical activation processes. The combination of modified electrodes and organic electrolytes can produce ultracapacitor-forming electrodes. The combination of surface heteroatoms in carbon nanomaterials has shown results in energy storage in ultracapacitors. The performance of carbon-heteroatom functional materials in the form of sulfur, phosphorus, and boron to nitrogen additives can be applied for energy storage [5]. Furthermore, the objectives to be achieved from this research are to analyze the effect of nitrogen addition on the results of characterization of bovine bone activated carbon and to analyze the effect of the type of electrolyte combined with nitrogen-doped bovine bone activated carbon electrodes on the performance of the ultracapacitor.

2. Method

2.1. Materials

The materials used include bovine bones (not edible) from the bovine cattle production center in Kalisidi Village, Semarang Regency. Other ingredients are urea, distilled water, HCl, KOH, H₂SO₄ obtained from e-brand, TEABF₄/AN, PTFE, filter paper, universal pH, fiberglass membrane, aluminum foil, jumper cable, PCB, resistor, diode, push-button.

24 2.2. Preparation of N-doped porous carbons

The production of nitrogen-doped porous activated carbon can be done by washing the cow bone waste, cutting it into 1-2 cm lengths, drying it at 200°C, then crushed into smaller materials. The dried bovine bone material was carbonized at 700°C for 1 hour under a nitrogen atmosphere with a flow rate of 1 L/min and a heating rate of 5°C/min, and carbon was produced [13]. Carbon increased the number of functional groups with nitrogen obtained from urea. Chemical activation on carbon, using KOH as an activating agent and urea as a nitrogen source. Comparison between activated carbon precursors, KOH, and urea in a weight ratio of 1: 2: X (X = 0, 1, 2 or 3) as NKACX. The mixture was dissolved in 100 mL of distilled water and stirred for 1 hour at room temperature. The sample was heated at 200°C for 4 hours. Furthermore, 1 M HCl solution and distilled water neutralized the remaining KOH solution and organic compounds by washing to pH 7. The activated carbon was then dried at 150°C for 5 hours. Next is NKAC0 carbon sample. NKAC1, NKAC2, and NKAC3 were analyzed to determine their ability.

2.3. Material characterization

After the activated carbon was successfully made, it was continued to characterize the functional groups contained in the sample and investigated using the Fourier Transform Infrared Spectrometer (FTIR, Thermo scientific Nicolet iS-10). The Brunauer–Emmett–Teller (BET) method was used to assess the specific surface area and pore size using a surface and pore size analysis instrument (BET, Surface Area and Pore Size Analyzer Quantachrome Nova 4200e) at 77.3 K. Morphology and microstructure of the material, characterized by Scanning Electron Microscopy (SEM, Jeol JSM-IT200) equipped with X-Max20 Energy Dispersive X-Ray Spectroscopy (EDS). The samples' crystal properties and phase purity were investigated by powder X-ray diffraction (XRD, Smartlab Rigaku X-Ray Source Copper, Cu).

2.4. Electro chemical characterization

The electrodes were made with a formulation of doped activated carbon as the active ingredient (80 wt.%), carbon black (10 wt.%), and polytetrafluoroethylene (PTFE, ten wt.%) in an aqueous solvent. After drying under infrared light, the mixture was pressed into disks (diameter of 10 mm, under a pressure of 6 MPa). The disc was then pressed with nickel foam as a current collector at 8 MPa for 1 min. The types of electrolytes used are HCl, KOH, and TEABF₄/AN.

Electrochemical performance analysis was obtained utilizing a multimeter, cyclic voltammetry (CV), and galvanostatic charge-discharge (GCD). Electrochemical testing was carried out using a standard electrode system as a comparison by using a Hg/HgO electrode as a reference electrode and a platinum electrode as a counter electrode in a 6 M KOH electrolyte solution at 25°C.

The Galvanostatic charge-discharge curve calculates specific capacitance based on equation (1). In the electrode device, the energy density (E, Wh/kg) equation (2), power density (P, W/kg) of the cell is calculated in equation (3).

$$C_{sp} = \frac{I \Delta t}{m \Delta V} \quad (1)$$

$$E = \frac{C_{sp} (\Delta V)^2}{2 \times 3.6} \quad (2)$$

$$P = \frac{E \times 3600}{\Delta t} \quad (3)$$

Where C_{sp} (F/g) represents the specific capacitance, I (A) is the Galvanostatic charge-discharge current, t (s) is the discharge time, m (g) is the mass of the electrode material, and V (V) is the change in discharge voltage so that the value of high-performance analysis is obtained at specific capacitance, voltage, and minimum value on the strong current. After being analyzed, the ultracapacitor with high specifications is obtained.

3. Result and Discussion

3.1. Physical and Chemical Properties of Materials

Table 1 describes data of the characterization of the activated carbon of the bovine bone

Table 1. The data of the characterization of the activated carbon of the bovine bone

Parameter	Carbon Sample		
	Carbon	KAC	NKAC
Yield (%)	81.8	95.7	91.9
Water content (%)	4.8	4.6	4.4

The activated carbon characterization process used five samples, namely AC, KAC, NKAC1, NKAC2, NKAC3, to determine the optimal condition of each sample. Table 1 can be seen that the results of characterization of activated carbon from bovine bones have the most significant yield in the KAC sample of 95.68%, while in NKAC, the results are lower than the KAC sample due to the washing and carbon filtering process, which is carried out repeatedly so that there is some carbon dissolved or wasted actives [14]. At the same time, the AC sample of 7.9% owns the highest water content. The binding of

water molecules by the activator will increase the adsorption ability of the activated carbon of bovine bone [15]. The low water content in the NKAC sample was caused by a combination of activation and doping processes because in this process, washing greatly affects the particle size, which causes the water content of activated carbon to decrease [14].

3.2. Characteristics of electrode material

The effect of heat treatment temperature and urea doping on the surface composition of carbonaceous materials was investigated by FTIR. The samples were examined qualitatively. Figure 1 shows the FTIR spectrum of urea-doped bovine bone carbon. The spectrum that appears as a peak is the carbonate group (890 cm^{-1}), phosphate (552 and 1012 cm^{-1}), C=C aromatic (1450 cm^{-1}), C=N (1675 cm^{-1}) and NH (3490 cm^{-1}). In addition, between 897 - 976 cm^{-1} , there is a strain bond between carbonate and hydroxide. The phosphate group with a wavenumber of 564 cm^{-1} has a bending vibration bond, while a stretching vibration bond is at a wavenumber of 1036 cm^{-1} [4]. In addition, the relative peak strength at 564 cm^{-1} on the phosphate was also associated with the OH bending vibration. The results show general bonds associated with organic compounds, namely C=O bonds, and O-H bonds. In this case, most organic compounds were removed after the doping treatment because the peak in the organic compound band was not detected. In 3497 cm^{-1} , crystalline powder was produced with the characteristic stretching mode of the N-H band. Where the N-H group comes from urea and the P-O group comes from the hydroxyapatite of bovine-bone. It can be attributed to the deformation of water molecules adsorbed on the surface of the sample so that it shows the state of urea in the carbon to form bonds with hydrogen and carbon [18], which can be doping heteroatoms doping carbon surface area. Based on the characterization results, during the heat treatment to obtain nitrogen-doped carbon, previously an elimination reaction to reduce hydrogen-containing groups, namely C-OH, C-H, and C-NH, reacted to form C=O, a nitrogen group [13]. Figure 1 depicts FTIR spectrum of Urea-doped bovine bone activated carbon.

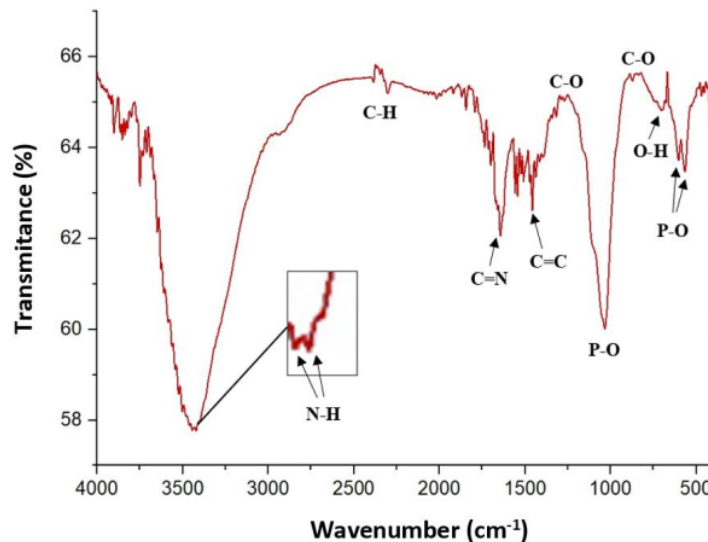


Figure 1. FTIR spectrum of Urea-doped bovine bone activated carbon

XRD spectroscopy was used to investigate the crystallographic structure of carbon-based materials, as illustrated in Figure 2. The results showed an increase in peak intensity and a decrease in peak width, indicating increased crystallinity and crystal size. The shift in the peak position is observed from the

standard position. The results show a dihydroxy process in hydroxyapatite during heating at 700°C for 1.5 hours so that the diffraction peak can be said to be under the crystal structure of hydroxyapatite [16]. In addition, NKAC showed a gradual increase in peak intensity when compared to AC and NAC. This affects the presence of larger carbon materials in the inorganic structure of carbon [17]. X-ray analysis also confirmed the graphite formation and amorphous [21] slightly crystalline nature of each sample. In addition, the high intensity at lower diffraction angles is due to the presence of micropores in the carbon network [21]. Surface area and pore volume of activated carbon sample is shown in Table 2.

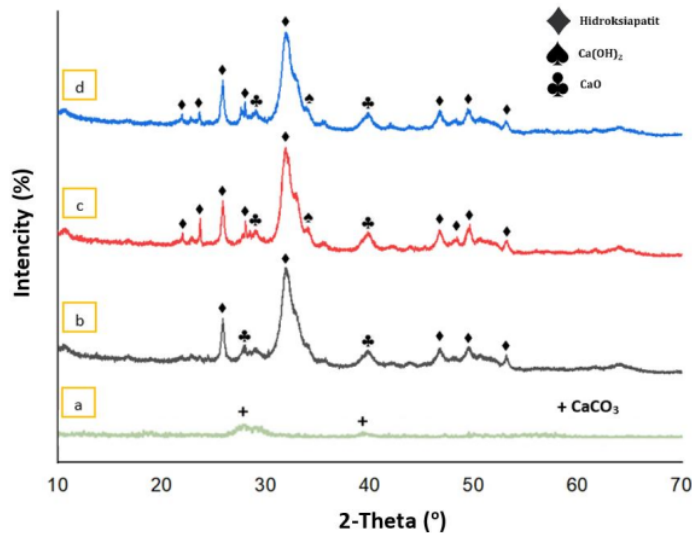
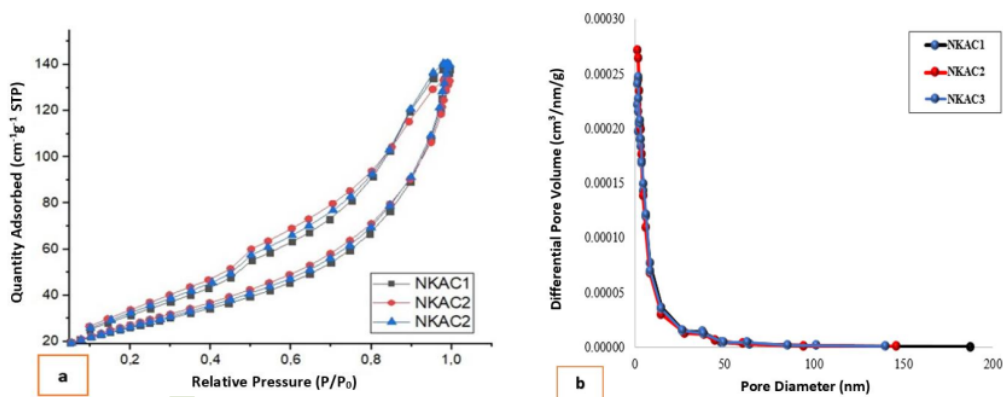


Figure 2. Comparison of sample diffraction patterns a) Bone Powder, b) Carbon, c) KAC, d) NKAC.

Table 2. Surface Area and Pore Volume of Activated Carbon Sample

Carbon	Surface Area (m ² /g)	Pore Volume (cm ³ /g)	Pore size (Å)
NKAC1	940.2	0.213	45.3
NKAC2	1001.0	0.206	40.7
NKAC3	972.3	0.217	44.5

The specific BET surface areas of NKAC1, NKAC2, and NKAC3 were 940.2 m²g⁻¹, 1001.0 m²g⁻¹, 972.3 m²g⁻¹, respectively (Table 2). At the same time, the pore volumes of these samples were 0.213 cm³g⁻¹, 0.206 cm³g⁻¹, and 0.217 cm³g⁻¹, respectively, which indicated that the functional group of nitrogen was optimal and the larger the surface area, the greater the adsorption-desorption ability of ions in electrons [7]. The formation of an electrical double layer on the electrodes and electrolytes can provide space to store more energy supported by functional groups that bind energy optimally [6]. So that NKAC2 which has a high surface area, is expected to produce a high specific capacitance [6]. These results indicate that doped N can increase the specific surface area of carbonaceous materials. In addition, the pore size distribution (PSD) of this sample has an average of 4.35 nm, where these pores include small mesopores (ranging from 4.0 nm to 4.5 nm). These results indicate that urea additive plays an essential role in producing pore. Porous materials with the high specific surface area are advantageous for application as active electrode materials for energy storage due to their fast mass charge transfer and ion diffusion [11]. Nitrogen adsorption-desorption and pore diameter curve is shown in Figure 3.



46 **Figure 3.** a) Nitrogen Adsorption-Desorption b) Pore Diameter Curve.

4 Apart from doped nitrogen heteroatoms, the specific surface area and pore size distribution of materials are essential factors in the field of carbon-based electrochemical capacitors. The performance of N-PC was further evaluated by measuring the nitrogen adsorption isotherm. Figure 3a shows the nitrogen adsorption-desorption curves of NKAC1, NKAC2, NKAC3, showing a steeply increasing curve at a low P/P₀ Range. The hysteresis loop's shape indicates an abundance of slit-shaped pores in these shale samples despite the differences in particle size [5]. In addition, a continuous increase in the high P/P₀ range indicates the presence of voids. In addition, NKAC2 shows a larger specific surface area (1001.0 m²/g) and total pore volume, which supports an increase in the adsorption capacity [12].

The pore size distribution of the material was also analyzed by the BJH method (Figure 3b), and the pore size distribution was about 4 nm. It is clear from the Figure 3b that the sample contains many mesopores. The large micropore structure can shorten the distance between the electrode surface and the ion center and increase the charge transfer rate. Many mesoporous structures can provide a channel for electrolyte transfer to increase the effective contact between the electrolyte and the electrode, thereby improving the energy storage performance of the material [7].

SEM studied the microstructure of the material. Figure 4 shows the microscopic topography of NKAC2 of the prepared nitrogen-doped porous carbon material showing the pore structure formed on the sample surface. Pore structure and smooth surface (Figure 4a-b). There are mesopores on the sample surface and pore structures that can increase the efficiency of electrochemical reactions. Mesoporous and interconnecting carbonaceous materials provide clear pathways for the transport and penetration of electrolyte ions, essential for rapid ion transfer [7].

The presence and uniform distribution of C, P, and O were observed on the NKAC2 surface, using SEM-EDX (Figure 4c-e). The elemental composition consists of 48.47% carbon, 40.70% oxygen, and 10.84% phosphorus. The phosphorus atom comes from hydroxyapatite which is owned by bone [20]. Based on the characterization results of bovine bone functional groups OH⁻, PO₄³⁻, and CO₃²⁻, where these groups are characteristics possessed by hydroxyapatite and bovine bone has a reasonably high crystallinity [18].

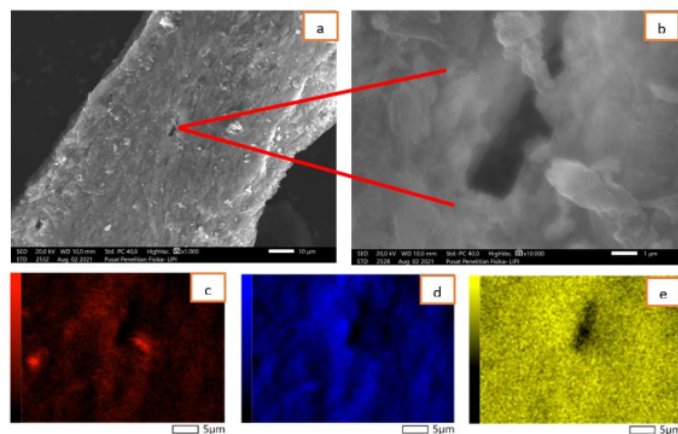


Figure 4. SEM-EDX activated carbon doping with urea a) morphology magnification 1000x, b) morphology magnification 10,000x, c) distribution of carbon content, d) Oxygen, e) Phosphorus.

3.3. Electrochemical performance of electrode material

The high surface area, large pore volume, interconnected porous structure, and nitrogen doping of the obtained samples were further investigated for their capacitance properties. The electrochemical performance of NKAC2 as the synthesized electrode was evaluated using cyclic voltammetry (CV), galvanostatic charge-discharge (GCD). Electrolyte ion diffusion rate on the ultracapacitor electrode was obtained from CV testing at various rates. These two tests were used to study the electrochemical evaluation of the synthesized activated carbon fiber ultracapacitor performance. The ultracapacitor cells were assembled in different electrolytes, with various potential windows from -0.2 to 1 V for the electrolytes of 1 M KOH, 1 M H_2SO_4 , and 1 M TEABF₄. The CV curve of the electrode under the same voltage window was examined at a scan rate of 25 mV/s. Measurement of GCD at the potential used is 0 to 1 V for electrolytes of 1 M KOH, 1 M H_2SO_4 , and 1 M TEABF₄.

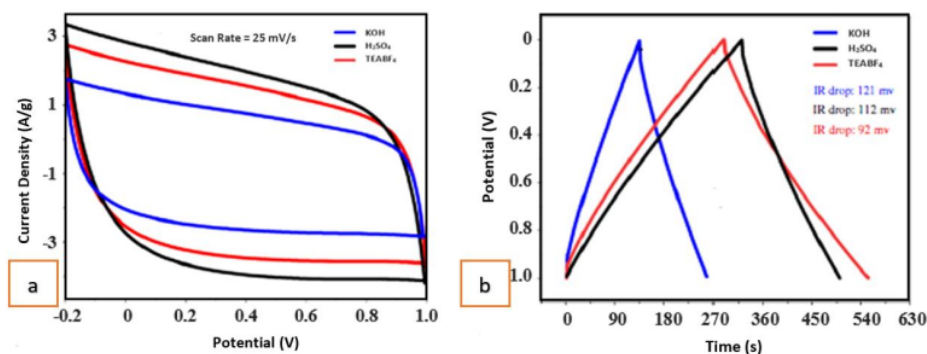


Figure 5. Electrochemical Testing of Cattle Bone Activated Carbon Electrodes a) Cyclic Voltammetry curve, b) Galvanostatic charge-discharge curve.

The specific capacitance of the electrode can be seen from the voltage and current curves obtained. The larger the area of charge and discharge current of cyclic voltammetry, the greater the specific capacitance value. The value of charge and discharge current from the electrode can be known from the

voltammogram obtained so that the specific capacitance value can be calculated. The test results in Figure 5a show that the ultracapacitor can move reversibly in a voltage of 0.2 to 1.0 Volt in the voltammetry test, while the GCD uses a voltage of 0 to 1 Volt. The CV curve maintains a rectangular shape at high scanning rates (25 mV/s), indicating the excellent level of capability of the carbon material. However, the slightly spindle-shaped CV curve for all carbon samples indicates a limited kinetic of electrolyte ions entering the smaller pores [19].

Analysis of the ultracapacitor charge-discharge time was carried out by testing the GCD in a two-electrode system. The GCD curve in Figure 5b shows a perfect triangle with a slightly marked decrease. It exhibits fast ion transport across the pores of the material. The specific capacitance calculated GCD curve is 155 F/g, 254 F/g, and 292 F/g at a current density of 0.1 A/g with each electrolyte in KOH H₂SO₄ and TEABF₄. The results are slightly superior to the specific capacitance at current densities of 185 F/g at 0.5 A/g [11], 108 F/g at 9 A/g (EMIBTI electrolyte) [12], and 258 F/g, respectively. At 5 A/g [7] of the same material, but different methods and types of electrolytes. The sample exhibits a smaller specific capacitance, which indicates a structural effect on the electrochemical performance of carbon materials [19]. This phenomenon shows an excellent ultracapacitor effect through the nitrogen functional group. A recent study on the effect of nitrogen doping on the specific capacitance of capacitors has shown that incorporating Nitrogen atoms into carbon skeletons at different positions can result in better electrochemical activity [21].

4. Conclusion

This research includes investigations to manufacture activated carbon from bovine bone and ultracapacitor structures with organic electrolytes. Electrodes made from activated carbon of bovine bone have a yield of 91.9% and a water content of 4.4%. The characterization of carbon has a specific surface area of 1001 m²/g, with a uniform pore size distribution with a dominant size of 0.7 nm with the type of micropores. It was found to contain hydroxyapatite and graphene carbon, CaO, and CaOH. The functional groups of doped activated carbon are presented in phosphates, carbonates, hydroxyapatites, phenols, and aromatics. Performance testing of the electrodes of bovine bone carbon combined with organic electrolyte showed the highest value at 292 F/g with a resistance of 0.1 A/g. This easy biomass-based approach provides an alternative route for preparing N-doped carbon, a promising candidate for energy storage ultracapacitor applications.

References

- [1] Hatfield-Dodds S, Schandl H, Newth D, Obersteiner M, Cai Y, Baynes T, West J and Havlik P 2017 *J. Clean. Prod* **144** 403
- [2] Gopalakrishnan A, Sahatiya P and Badhulika S 2018 *ChemElectroChem* **5** 531
- [3] Jiang, J, Zhang Y, Nie P, Xu G, Shi M, Wang J, Wu Y, Fu R, Dou H and Zhang X 2018 *Adv. Sustain. Syst* **2** 17001
- [4] Ghosh S, Santhosh R, Jeniffer S, Raghavan V, Jacob G, Nanaji K, Kollu P, Jeong S K and Grace A N 2019 *Sci. Rep.* **9** 1
- [5] Abbas Q, Raza R, Shabbir I and Olabi A G 2019 *J. Sci. Adv. Mater. Devices* **4** 341
- [6] Zhang H, Zhang L, Chen J, Su H, Liu F and Yang W 2016 *J. Power Sources* **315** 120
- [7] Niu J, Shao R, Liang J, Dou M, Li Z, Huang Y and Wang F 2017 *Nano Energy* **36** 322
- [8] Syamberah, Anita S and Hanifah A 2015 *JOM FMIPA* **2** 38
- [9] Mohammed A, Aboje A A, Auta M and Jibril M 2012 *Adv. Appl. Sci. Res.* **3** 3089
- [10] Wardani S and Rosa E 2018 *J. Serambi Engineering* **3** 308
- [11] Huang W, Zhang H, Huang Y, Wang W and Wei S 2011 *Carbon* **49** 838
- [12] Goodman P A, Li H, Gao Y, Lu Y F, Stenger-Smith J D, Redepenning J 2013 *Carbon* **55** 291
- [13] Rengga W D P, Triwibowo B, Putra J T, Nugroho A, Kadarwati S and Subiyanto S 2021 *Trans. Tech. Publ. Ltd.* **324** 125
- [14] Aryani F, Mardiana F and Wartomo 2019 *IJMLST* **1** 16

- [15] Previanti P, Sugiani H, Pratomo U and Sukrido S 2015 *JCNA* **3** 48
- [16] Cascarosa E, Ortiz M C, Sánchez J L, Gea G and Arauzo J 2012 *Biomass Bioenergy* **40** 190
- [17] Rojas-Mayorga C K, Silvestre-Albero J, Aguayo-Villarreal I A, Mendoza-Castillo D I and Bonilla-Petriciolet A 2015 *Micropor. Mesopor. Mat.* **209** 38
- [18] Yala S, Khireddine H, Sidane D, Ziani S and Bir F 2013 *J. Mater. Sci.* **48** 7215
- [19] Chu M, Li M, Han Z, Cao J, Li R and Cheng Z 2019 *R. Soc. Open Sci.* **6** 190132
- [20] Afifah F and Cahyaningrum S E 2020 *UNESA J. Chem* **9** 189
- [21] Yang X, Wang Q, Lai J, Cai Z, Lv J, Chen X, Chen Y, Zheng X, Huang B and Lin G 2020 *Mater. Chem. Phys.* 123201

Acknowledgement

We are grateful for funding from the Directorate General of Higher Education, Ministry of Education, and Culture, Research, and Technology, and the Laboratory at Universitas Negeri Semarang in implementing the Exact Research-Student Creativity Program in 2021 with No. 1686 /E2/TU/2020.

Preparation and characterization of activated

ORIGINALITY REPORT

19%

SIMILARITY INDEX

14%

INTERNET SOURCES

16%

PUBLICATIONS

5%

STUDENT PAPERS

PRIMARY SOURCES

- 1 repository.futminna.edu.ng:8080 1%

Internet Source
- 2 Wenqiang Hu, Jianyu Huang, Peifeng Yu, Mingtao Zheng, Yong Xiao, Hanwu Dong, Yeru Liang, Hang Hu, Yingliang Liu. " Hierarchically Porous Carbon Derived from for Electrochemical Capacitance and Hydrogen Storage ", ACS Sustainable Chemistry & Engineering, 2019 1%

Publication
- 3 Manavalan Vijayakumar, Ravichandran Santhosh, Jyothirmayi Adduru, Tata Narasinga Rao, Mani Karthik. "Activated carbon fibres as high performance supercapacitor electrodes with commercial level mass loading", Carbon, 2018 1%

Publication
- 4 mdpi-res.com 1%

Internet Source
- 5 Gunawan, Amir Arifin, Irsyadi Yani, Sufran Dinar Arian. " The Fabrication Porous 1%

Scaffold Using Sweet Potato Starch as a Natural Space Holder ", Journal of Physics: Conference Series, 2019

Publication

6	sportdocbox.com Internet Source	1 %
7	www.rsc.org Internet Source	1 %
8	"Preface", Journal of Physics: Conference Series, 2021 Publication	1 %
9	lppm.itsb.ac.id Internet Source	1 %
10	"Porous Materials", Springer Science and Business Media LLC, 2021 Publication	<1 %
11	coek.info Internet Source	<1 %
12	D N K P Negara, T G T Nindhia, I W Surata, M Sucipta, F Hidajat. "Activated carbon characteristics of tabah bamboo that physically activated under different activation time", IOP Conference Series: Materials Science and Engineering, 2019 Publication	<1 %
13	Submitted to Middle East Technical University Student Paper	<1 %

14	doaj.org Internet Source	<1 %
15	open.library.ubc.ca Internet Source	<1 %
16	Kavitha Ramadass, C. I. Sathish, Sujanya MariaRuban, Gopalakrishnan Kothandam et al. " Carbon Nanoflakes and Nanotubes from Halloysite Nanoclays and their Superior Performance in CO Capture and Energy Storage ", ACS Applied Materials & Interfaces, 2020 Publication	<1 %
17	ddd.uab.cat Internet Source	<1 %
18	assets.researchsquare.com Internet Source	<1 %
19	bioresources.cnr.ncsu.edu Internet Source	<1 %
20	"Production of Materials from Sustainable Biomass Resources", Springer Science and Business Media LLC, 2019 Publication	<1 %
21	Jiaming Bai, Songbo Mao, Feiqiang Guo, Rui Shu, Sha Liu, Kaiming Dong, Youjin Yu, Lin Qian. "Rapeseed meal-derived N, S self-codoped porous carbon materials for	<1 %

supercapacitors", New Journal of Chemistry,
2022

Publication

22

trilhasdahistoria.ufms.br

Internet Source

<1 %

23

Yajun Ji, Yalei Deng, Hongmei Wu, Zhixiang Tong. "In situ preparation of P, O co-doped carbon spheres for high-energy density supercapacitor", Journal of Applied Electrochemistry, 2019

Publication

<1 %

24

Yuxin Tian, Haifeng Zhou. "A novel nitrogen-doped porous carbon derived from black liquor for efficient removal of Cr(VI) and tetracycline: Comparison with lignin porous carbon", Journal of Cleaner Production, 2022

Publication

<1 %

25

www.frontiersin.org

Internet Source

<1 %

26

www.mdpi.com

Internet Source

<1 %

27

Mingyun Guan, Guoxing Zhu, Tongming Shang, Zheng Xu, Jianhua Sun, Quanfa Zhou. "PVP-mediated synthesis of MPO₄ (M = Y, Er) hollow mesocrystal cubes via a ripening process", CrystEngComm, 2012

Publication

<1 %

28

Yuru Ge, Md. Ikram Ul Hoque, Qunting Qu. "1D Hematite-[α -Fe₂O₃]-nanorods prepared by green fabrication for supercapacitor electrodes", *Electrochemical Energy Technology*, 2019

Publication

<1 %

29

Zhang, Gaini, Lijun Ren, LingJuan Deng, Jianfang Wang, Liping Kang, and Zong-Huai Liu. "Graphene-MnO₂ nanocomposite for high-performance asymmetrical electrochemical capacitor", *Materials Research Bulletin*, 2014.

Publication

<1 %

30

article.sciencepublishinggroup.com

Internet Source

<1 %

31

Jinru Yue, Bo Li, Tao Ju, Zongrong Ying, Jiating Lu, Yongzheng Zhang. "Polyhedron carbon-scale stacking foldable fibrous film electrode with high capacitance performance from chitin fiber cloth for super flexible supercapacitors", *Materials Research Express*, 2018

Publication

<1 %

32

fisika.lipi.go.id

Internet Source

<1 %

33

www.pertanika.upm.edu.my

Internet Source

<1 %

34

Zijian Zhao, Yong Wang, Min Li, Ru Yang. "High performance N-doped porous activated carbon based on chicken feather for supercapacitors and CO capture ", RSC Advances, 2015

Publication

<1 %

35

mostwiedzy.pl

Internet Source

<1 %

36

sciendo.com

Internet Source

<1 %

37

www.mrs-j.org

Internet Source

<1 %

38

C.K. Rojas-Mayorga, J. Silvestre-Albero, I.A. Aguayo-Villarreal, D.I. Mendoza-Castillo, A. Bonilla-Petriciolet. "A new synthesis route for bone chars using CO₂ atmosphere and their application as fluoride adsorbents", Microporous and Mesoporous Materials, 2015

Publication

<1 %

39

Diego Ramón Lobato-Peralta, Estefanía Duque-Brito, Heidi Isabel Villafán Vidales, Adriana Longoria et al. "A review on trends in lignin extraction and valorization of lignocellulosic biomass for energy applications", Journal of Cleaner Production, 2021

Publication

<1 %

40 Hua-Guang Yu, Jia-Xin Dong, Yi Liu, Song-Sheng Qu. " Standard Enthalpies of Formation of [Ln(Gly) (H O)]Cl ·2H O (Ln = Pr, Nd; Gly = Glycine): A Calorimetric Study ", Journal of Chemical & Engineering Data, 2003
Publication <1 %

41 dspace.nm-aist.ac.tz
Internet Source <1 %

42 kaihangshi.github.io
Internet Source <1 %

43 nanocenter.nankai.edu.cn
Internet Source <1 %

44 pubs.acs.org
Internet Source <1 %

45 research.usq.edu.au
Internet Source <1 %

46 rlhxxb.sxicc.ac.cn
Internet Source <1 %

47 scholar.sun.ac.za
Internet Source <1 %

48 www.science.gov
Internet Source <1 %

49 Murray, S., M. Trudeau, and D. M. Antonelli. "X-ray Photoelectron Spectroscopy and Magnetic Studies on the Effect of Pore Size, <1 %

Wall Thickness, and Wall Composition on Superparamagnetic Cobaltocene Mesoporous Nb, Ta, and Ti Composites", Inorganic Chemistry, 2000.

Publication

50

eprints.utm.my

Internet Source

<1 %

51

Mei Li, Shisen Xiang, Xiaoqing Chang, Chengshuai Chang. "Resorcinol-formaldehyde carbon spheres/polyaniline composite with excellent electrochemical performance for supercapacitors", Journal of Solid State Electrochemistry, 2016

Publication

52

Rong Shao, Jin Niu, Jingjing Liang, Mengyue Liu, Zhengping Zhang, Meiling Dou, Yaqin Huang, Feng Wang. "Mesopore- and Macropore-Dominant Nitrogen-Doped Hierarchically Porous Carbons for High-Energy and Ultrafast Supercapacitors in Non-Aqueous Electrolytes", ACS Applied Materials & Interfaces, 2017

Publication

<1 %

Exclude quotes Off

Exclude matches Off

Exclude bibliography On

Preparation and characterization of activated

GRADEMARK REPORT

FINAL GRADE

/0

GENERAL COMMENTS

Instructor

PAGE 1

PAGE 2

PAGE 3

PAGE 4

PAGE 5

PAGE 6

PAGE 7

PAGE 8

PAGE 9

PAGE 10
